Plasma actuated heat transfer

Subrata Roy[a] and Chin-Cheng Wang
Computational Plasma Dynamics Laboratory and Test Facility, Mechanical and Aerospace Engineering, University of Florida, Gainesville, Florida 32611-6300, USA

(Received 10 April 2008; accepted 13 May 2008; published online 12 June 2008)

We introduce plasmas for film cooling enhancement in gas turbines and other engineering applications. We identify mechanisms to actuate essentially stagnant fluid just downstream of the cooling hole by employing three-dimensional body force for different hole geometries. Such methods actively alter flow structures in the vicinity of an actuator using an electrodynamic mechanism that induces attachment of cold jet to the work surface. Numerical results are compared with published experimental data and other numerical predictions for the latest film cooling technology. An effectiveness improvement of above 100% over the standard baseline design is predicted. © *2008 American Institute of Physics*. [DOI: 10.1063/1.2938886]

Cooling of hot surfaces with cold fluid film is commonplace in many engineering problems including vertical/short takeoff and landing and gas turbine blades. For example, in gas turbine blades, such fluid film based cooling becomes mandatory to protect them from high thermal stresses induced by hot combustion gases and thus increasing blade lifetime. In this process, cold gas is injected from a row of holes located spanwise into the hot crossflow creating a three-dimensional flow field entraining some hot gas to bend toward the blade. There is plenty of research in traditional means to control the flow path such that the cold fluid remains attached to the surface while spreading in the crosswise direction to cover the entire span.[1] Figure 1(a) represents a geometry which has been extensively investigated[2,3] for cooling performance for a wide range of blowing ratio (i.e., momentum ratio of injected air to crossflow). Note that with higher momentum ratio, the film cooling effectiveness is ultimately limited by temporary lift off of the cold fluid as it ejects out of the slanted hole.[4] There are methods such as shaped holes that reduce this lift off.[5] Such methods are effective for a particular blowing ratio but they cannot actively adjust to varying turbine loads. Also the complex dynamic nature of the film cooling flow makes it necessary to actively control it with a dynamic force that varies temporally and spatially working with the dominant turbulence scales. Both pulsed dc and ac powered plasma actuators can induce such active control[6] over the dynamics of film cooling in an instantaneous manner. The actuator can be of the form as shown in Fig. 1(b) where the powered and grounded electrodes are kept at a sequence to push the fluid in the forward direction. Such configurations are based on documented numerical experience and experimental evidence.[7] The induced force in such actuators is local (within a few millimeters) and dissipates quickly outside the domain of influence as shown in Fig. 2 schematic below. The momentum transfer between the plasma and gas happens due to collisional momentum transfer between charged ions and neutral atoms. High freestream gas temperature will enhance dissociation and hence help plasma generation due to ionization in the vicinity of the electrodes. Such actuation does not require any mechanical parts, and the actuator electrode sets can be applied as a patch on the surface of the existing ceramic coating of the turbine blade or embedded into the coating.

This letter explores mechanism for such active control. Figure 1(c) shows schematics of various hole shapes: A for baseline, B for bumper with $0.5d$ height, C for jet hole with compound slopes, and D for rectangular slot. The intension of the shapes B and D is to trip the emerging cold jet. We introduce the concept, as described in Fig. 2. Here we use plasma actuator at the downstream (or upstream) of the cooling hole. Such actuators are made of a set of electrode pairs, as shown in Fig. 1(b), between which electric potential and induced weak ionization of the working gas generate an electric body force that is dominant inside the boundary layer. In such an actuator because of geometry, the electrohydrodynamic body force field is three-dimensional. The induced flow actuation is directly linked with the gas-charged particle interaction and thus instantaneous.[6,7] The discharge from the upstream electrode [Fig. 1(b)] is powered with a pulsed dc voltage of $\phi=\phi_0 \sin^4(2\pi kt)$ volts with $\phi_0=1000$ V, and $k=5$ kHz. The powered electrode is located in a quadrant just downstream of the cooling hole exit. The grounded electrode is situated at a uniform 2 mm gap downstream of the powered electrode. One may further reduce the voltage by reducing the gap such that the electric field is of the same order (above 30 kV/cm). Based on the knowledge gained from the first principles model for air,[8] we approximate induced body force as an exponentially decaying distribution with its peak just downstream of the cooling hole exit.

We apply the time average of the electric force. This is allowable due to largely disparate timescales of plasma and gas flow. Also, due to geometric change (elliptic as compared to straight electrode arrangement), the actuator force density is represented by a slightly modified version as $\mathbf{F}=+6F\hat{i}-3F\hat{j}\pm F\hat{k}$, where $F=\Lambda f_x f_y f_z$ with $f_x=[(x-d/2)^2+C_1]/C_2$, $f_y=[\exp(-1000y)/C_3]-C_4$, $f_z=[(z-d/2)^2+C_5]/C_6$. The amplitude Λ is varied as 0, 2, and 2000 kN/m^3 for $C_1=1.5\times10^{-6}$, $C_2=3.09\times10^{-6}$, $C_3=0.98$, $C_4=0.057$, $C_5=1.58\times10^{-6}$, $C_6=3.14\times10^{-6}$. Depending on the actuation device a local kN/m^3 force density may be obtained by spending a few watts[6,8] for $\Lambda=2$ kN/m^3 to kW s for $\Lambda=2000$ kN/m^3. Note that this is a small fraction ($<1\%$) of the turbine power which may eventually reduce the energy budget by more effective cooling.

[a]Electronic mail: roy@ufl.edu.

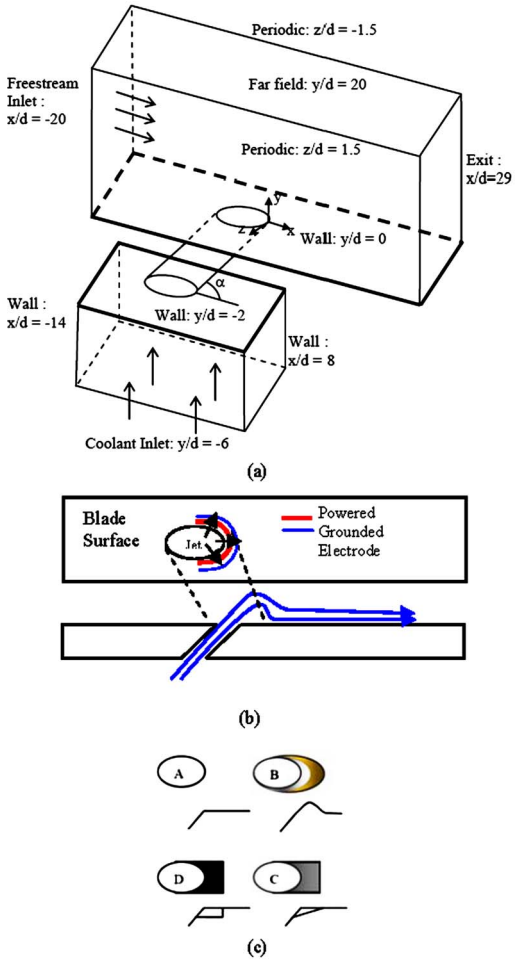

FIG. 1. (Color online) Problem schematic for heat transfer actuation. (a) Film cooling simulation geometry, (b) adiabatic flat plate with actuator, and (c) cooling hole types A–D.

The film cooling performance is measured by an effectiveness parameter $\eta(x,y)=[T_{\mathrm{fs}}-T_s(x,y)]/(T_{\mathrm{fs}}-T_j)$, where $T_s(x,y)$, T_j, and T_{fs} are the work surface (x,y), cooling jet, and hot freestream gas temperatures, respectively. The effectiveness is plotted against a nondimensional location x/Md, where x is the downstream distance, $M=\rho_j u_j/\rho_f u_f$ is the blowing ratio, and d is the slot (hole) diameter. The density ρ_j and velocity u_j of the fluid at the jet exit plane are related to the freestream density ρ_f and velocity u_f such that $\rho_j/\rho_f=Mu_f/u_j$. As compared to the slots, a row of discrete holes typically has a much lower span averaged downstream film effectiveness distribution for the same x/Md $(=x/d$ for $M=1)$ due to the formation of vortices which allow hot gas to penetrate to the wall. These vortices are of the scale of the hole size and smaller. We identify η_c as the centerline effectiveness and η_s as the spanwise averaged effectiveness for convenience. All cases discussed here use a moderate blowing ratio $M=1$ for $\alpha=35°$ and a freestream velocity of 114 m/s, a density ratio of freestream to cold jet of 0.5. The Strouhal number, $\mathrm{Sr}=kd/(\sin\alpha)u_f$, based on the free stream flow velocity is 0.2. Hence, the large-scale flow instabilities are nearly independent of the flow Reynolds number. Note that the pure convection related flow frequency, $u_f(\sin\alpha)/d=22800$, is comparable to the frequency of the power driving the actuator. The unsteady effects of the pulsed voltage source are ignored considering that the charged species dynamics in the plasma are much faster than the fluid.

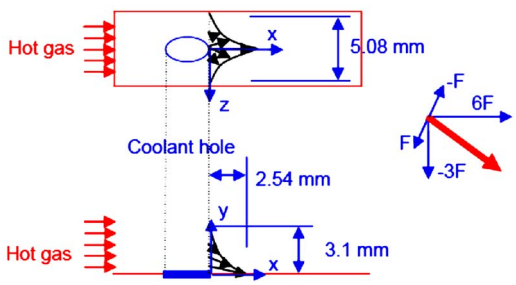

FIG. 2. (Color online) Time average of electrodynamic force distribution.

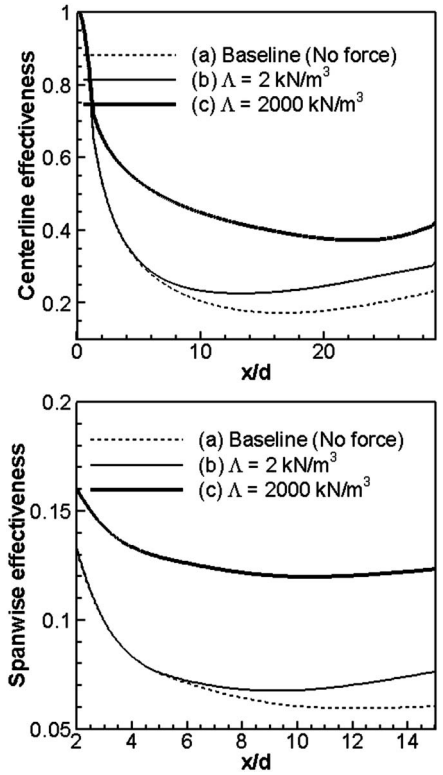

FIG. 3. Effect of plasma force on film cooling heat transfer. (a) Centerline effectiveness η_c and (b) spanwise averaged effectiveness η_s.

The effect of plasma discharge on the heat transfer near the work surface is compared in Fig. 3 for $\Lambda=0$ (plasma off), and $\Lambda=2$ and 2000 kN/m^3 (plasma on) for a standard slanted hole design A. In Fig. 3(a), the application of a small plasma force density of $\Lambda=2$ kN/m^3 caused η_c to rise from 0.17 to 0.22 (a 30% increase) at the normalized location of $x/d=15$. Interestingly, the bifurcation started beyond x/d

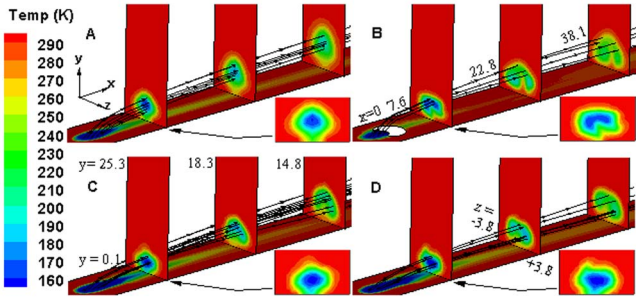

FIG. 4. (Color online) Temperature contours at spanwise plane $(x/d=3)$ for various designs A–D.

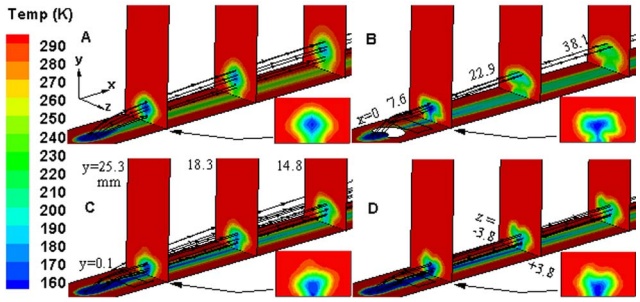

FIG. 5. (Color online) Temperature contours at spanwise plane (x/d=3) for designs A–D with actuation force density $\Lambda=2000$ kN/m^3.

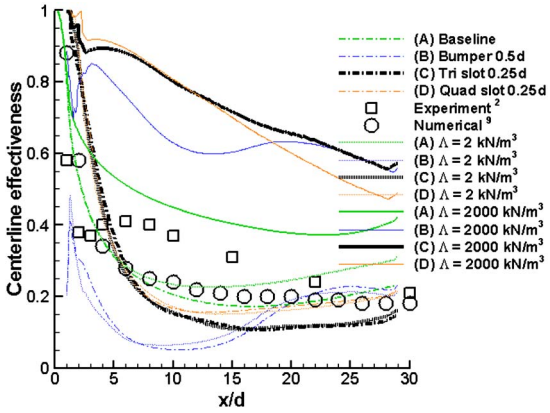

FIG. 6. (Color online) Effect of plasma actuation on centerline effectiveness.

=5. As we increase the plasma force density to $\Lambda=2000$ kN/m^3, η_c starts increasing rapidly beyond $x/d=1.5$. When we increase the force density until 2000 kN/m^3, the effectiveness shoots up from 0.17 ($\Lambda=0$) to 0.41 improving over 140%. In order to understand the spread of the cooling jet, the spanwise averaged effectiveness η_s is plotted in Fig. 3(b). Results show that for a small discharge ($\Lambda=2$) η_s increases from 0.06 to 0.076 (26% increase) at $x/d=15$. The effect goes up significantly for $\Lambda=2000$ to $\eta_s=0.125$ (108% increase). Such comparisons give us insight on how the cooling jet becomes wider and attaches to work surface as the fluid interacts with the local plasma discharge.

At downstream of the hole, the fluid trips outward (crosswise) and downward in B as compared to A, while in D the cooling jet essentially clings to the work surface. The typical single counter-rotating vortex pair in the baseline solution for A (not shown) has peak strength of about 20 000/s as cooling jet juts out. The weaker vortices move outward and away from the wall. For design B without plasma, the strength of vortex pair doubles to 40 000/s with a much larger core diameter. Application of plasma ($\Lambda=2000$) for B splits this single vortex pair into two separate counter-rotating vortex pairs with equal strength. For design D with plasma the single vortex pair has slightly lower strength (~35 000/s) with strong attachment toward the work surface inducing large dispersion of the cold jet. We infer that surface heat transfer may not only be improved by plasma force but also be further enhanced by local tripping of the jet as it emanates from the hole.

Figure 4 plots the temperature distribution on the same planar location ($x/d=3$) for no actuation $\Lambda=0$. At this distance the cold fluid lifts off in traditional design A. The situation worsens for B just beyond the bump. However, for C and D, the cold jet bends (trips) for modest improvement of the cooling region on the work surface. In contrast, the influence of plasma induced electric force can be significant, as seen in Fig. 5, for $\Lambda=2000$ kN/m^3. The temperature of the work surface reduced for all designs. Clearly for B, C, and D the cold jet attaches to the work surface the extent of which increases from B to C to D. It is thus essential to quantify the improvement in cooling performance.

Figure 6 plots the effect of plasma actuation on centerline effectiveness for four designs A–D. The computed η_c for the baseline case without plasma discharge ($\Lambda=0$) compares reasonably with the experimental data[3] and other previously reported numerical result.[9] The performance plots of different hole shapes show that C and D have better η_c before $x/d=6$ because the expansion of the jet reduces the momentum ratio increasing the cooling performance. Also the step at edge of D acts as a trip for the cold fluid inducing more attachment. Interestingly, case B provides higher η_c beyond $x/d=20$ because the jump effect delays the cold fluid attached to the work surface. The effect of small plasma actuation ($\Lambda=2$) is evident only for the case A beyond $x/d=5$ because the effect of the geometric modifications is higher than the plasma force density. As compared to without actuation ($\Lambda=0$), the η_c increases by over 70%, 558%, 137%, and 164% more, respectively, at $x/d=5$ as the force density increases to the maximum ($\Lambda=2000$) for designs A–D. It is evident that the plasma flow control guarantees the flow is attached to the surface improving the heat transfer drastically.

In conclusion, we explored the advantages of plasma based active heat transfer control for film cooling of a flat work surface. Results demonstrated advantages including three-dimensional dispersion of the cold jet over the work surface without any major loss in flow energy. Based on the numerical prediction, it is evident that application of plasma discharge along with modifications of the hole geometry can culminate into over 100% improvement of the film cooling effectiveness. There could be practical considerations for realistic blades in gas turbines such as surface oxidation of the electrodes and spallation. This needs to be investigated during *situ* testing, which is not in the scope of the present paper.

[1]D. Lakehall, G. S. Theodoridis, and W. Rodi, Int. J. Heat Fluid Flow **19**, 418 (1998); S. Roy, Numer. Heat Transfer, Part A **38**, 701 (2000); A. Sleiti and J. S. Kapat, J. Thermophys. Heat Transfer **20**, 67 (2006).
[2]S. Kapadia, S. Roy, and J. Heidmann, J. Thermophys. Heat Transfer **18**, 154 (2004).
[3]S. V. Ekkad, S. Ou, and R. B. Rivir, J. Turbomach. **128**, 564 (2006); H. Kruse, *Heat and Mass Transfer in Rotating Machinery* (Hemisphere, Washington, DC, 1984), p. 451–461; A. K. Sinha, D. G. Bogard, and M. E. Crawford, J. Turbomach. **113**, 442 (1991).
[4]J. H. Leylek and R. D. Zerkle, J. Turbomach. **111**, 358 (1994); V. K. Garg and D. L. Rigby, Int. J. Heat Fluid Flow **20**, 10 (1999); **21**, 134 (2000).
[5]D. G. Hyams and J. H. Leylek, J. Turbomach. **122**, 122 (2000); R. S. Bunker, J. Heat Transfer **127**, 441 (2005); S. Na and T. I.-P. Shih, *ibid.* **129**, 464 (2007).
[6]S. Roy, Appl. Phys. Lett. **86**, 101502 (2005); S. Roy and D. Gaitonde, Phys. Plasmas **13**, 023503 (2006).
[7]K. P. Singh and S. Roy, J. Appl. Phys. **102**, 013305 (2008); **103**, 103303 (2008).
[8]A. Labergue, L. Leger, E. Moreau, and G. Touchard, J. Electrost. **63**, 961 (2005).
[9]X. Z. Zhang and I. Hassan, J. Thermophys. Heat Transfer **20**, 754 (2006).